Safe and Adaptive Multi-Robot Formation Control via Composed CBFs in the Presence of Dynamic and Uncertain Obstacles

Tohid Kargar Tasooji   Ramviyas Parasuraman

***Abstract*— This paper introduces a decentralized control framework for safe and adaptive multi-robot formation in dynamic and uncertain environments. The proposed approach formulates a generalized quadratic program (QP) that integrates multiple Control Barrier Functions (CBFs) for safety, connectivity preservation, and obstacle avoidance with a Control Lyapunov Function (CLF) for goal convergence. To resolve inherent conflicts among these objectives, we present the first integration of behavior trees with CBF–CLF–QP control, providing a structured and modular mechanism for prioritized switching across safety, connectivity, formation, and goal-reaching tasks without deadlock. The proposed framework is fully decentralized, computationally efficient, and scalable, with each agent solving a local QP in sub-second cycles, making it practical for real-time, on-board implementation. Extensive simulations and experiments in cluttered, dynamic environments with moving obstacles and uncertain obstacle geometries demonstrate the method's ability to ensure safety, maintain network connectivity, and achieve resilient formation control while adapting to rapidly changing conditions.**

I. Introduction

The control of multi-robot systems (MRS) has attracted considerable attention over the past decades due to their inherent advantages in scalability, robustness to individual failures, and flexibility in performing complex tasks. Among the various coordination problems in MRS, formation control plays a central role, enabling agents to cooperatively achieve and maintain desired spatial configurations while navigating through dynamic and uncertain environments. Applications range from search-and-rescue missions [1], [2], to automated goods transport in warehousing [3], to coordinated field operations in precision agriculture. Maintaining prescribed inter-robot spacing is essential not only for ensuring collision-free operation and task coordination but also for preserving communication connectivity within the team.

However, real-world deployments introduce two fundamental challenges. First, multi-robot teams must operate in cluttered and dynamic environments populated with moving obstacles and objects whose geometry and motion are only partially observed and subject to uncertainty. Second, accomplishing mission objectives, such as ensuring safety, maintaining formations, preserving connectivity, and achieving goal convergence, requires resolving inherently conflicting requirements under decentralized information exchange and limited onboard computational resources.

School of Computing, University of Georgia, Athens, GA 30602, USA. Corresponding author email: ramviyas@uga.edu

This research is supported by the Army Research Laboratory and is accomplished under DCIST Cooperative Agreement W911NF-17-2-0181.

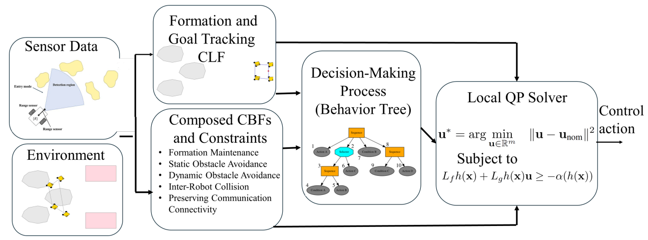

Fig. 1: Overall control architecture of the multi-robot formation control combining perception, composed constraints, and real-time optimization.

Control Barrier Functions (CBFs) [4] and Control Lyapunov Functions (CLFs) [5], composed within a Quadratic Program (QP), provide a principled framework to guarantee safety through forward-invariant sets while simultaneously pursuing task objectives. Such formulations are well-suited for real-time execution and have demonstrated formal safety guarantees and effective task performance. However, existing approaches assume static or parameterized obstacles and lack modular mechanisms to systematically resolve conflicts between multiple objectives, including safety, connectivity preservation, formation maintenance, and obstacle avoidance [6]. Moreover, current methods provide limited support for decentralized operation in environments with dynamic and uncertain obstacle geometries or partial observations.

We address these limitations by developing a decentralized, compositional CBF–CLF–QP framework (see Fig. 1 for an overview) for safe and adaptive multi-robot formation control in dynamic and uncertain environments. The proposed approach integrates multiple CBFs to enforce heterogeneous constraints—including inter-robot separation, connectivity preservation, and multi-class obstacle avoidance, together with a CLF for goal convergence in a unified, locally solved QP. To systematically resolve conflicts among objectives, we introduce a modular priority and switching mechanism based on behavior trees [7], which enables structured and deadlock-free transitions between safety, connectivity, formation, and goal-reaching behaviors.

Our main contributions are summarized below. *First*, we develop a hierarchical control framework that integrates behavior trees with CBF–CLF–QP-based control to enable modular and prioritized coordination among safety, connectivity preservation, formation maintenance, and goal-reaching objectives. Rather than treating these objectives independently, the proposed architecture provides a structured mechanism for switching and prioritizing them in multi-robot systems. *Second*, we formulate signed-distance-based CBF constraints for obstacle avoidance in environments containing static and dynamic polygonal obstacles with uncertain or partially observed geometries. These barrier constraints are incorporated into the QP layer to enforce safety while allowing the robots to continue pursuing formation and goal-reaching objectives. *Third*, the proposed solution guarantees scalability to large MRS teams by maintaining sub-second per-agent computation and restricting communication to local neighbors (i.e., distributed architecture). *Finally*, we validate the proposed framework through both simulation and hardware experiments on the Robotarium platform, demonstrating resilient formation control and robust performance in cluttered, dynamic environments.

II. Related Work

The use of CBFs for safety in MRS has gained significant attention in recent years. Prior works have addressed formation control and obstacle avoidance using CBF-based QPs in both centralized and decentralized settings. Several studies integrate CBFs with QPs to enforce safety while maintaining inter-robot constraints. For example, [4] develop CBF–QP formulations for rigid and elastic formations navigating unknown environments, validated through hardware experiments. However, these approaches typically assume static or simply parameterized obstacles and do not address uncertain, time-varying geometries under partial observability, nor do they provide modular decentralized conflict resolution among heterogeneous objectives. Similarly, distributed QP-based methods in [8], [9] ensure safety and navigation but often rely on known or fixed obstacle models.

Recent work has also explored CBFs for cooperative manipulation and payload transportation. In particular, [10] propose a CBF-based trajectory planner for multi-quadrotor cable-suspended payload transport, modeling system components as convex polytopes. While effective in cluttered environments, this framework focuses on centralized planning and convex obstacle representations, limiting applicability to decentralized, real-time control with nonconvex or partially observed environments. Affine formation control has been extensively studied in [11]–[13], providing strong guarantees for shape, scale, and orientation regulation. However, these approaches typically do not incorporate dynamic obstacle avoidance or real-time safety constraints.

More recently, compositional and hierarchical safety using Boolean logic over CBFs has been investigated in [6], [14]. These works establish a foundation for modular safety frameworks but assume fully known environments and controlled settings. Learning-based CBF construction, such as the Gaussian process framework in [15], improves adaptability in unknown environments but introduces challenges in real-time performance and model accuracy. The unification of safety and performance via CLF–CBF QPs was formalized in [16], ensuring forward invariance of safety sets while achieving control objectives.

Our work departs from prior CBF–QP approaches for multi-robot formation that either enforce safety and formation via rigid/elastic edges without an explicit high-level prioritization mechanism [4] or focus on distributed safe navigation without formation-keeping or a structured way to arbitrate between safety, connectivity, and goal tracking [8], [9], typically relying on fixed QP weights and static or simply parameterized obstacles. In contrast, we explicitly use a behavior tree (BT) to compose CBF–CLF–QP controller layers to realize a "hierarchy of needs" [6], [17] over safety, connectivity, formation (with slack/recovery), and goal convergence, where each layer is encoded as a time-varying CBF with smooth gating functions $\Phi(\cdot)$, yielding dynamic, state-dependent activation of constraints. Existing CBF-based formation and navigation methods also typically assume static, disc-shaped, or known convex obstacles—e.g., Pham et al. [4] and Pallar et al. [10], as well as compositional CBF works such as [6], [14] do not address uncertainty in the range-based perception of polygonal obstacles; our signed-distance CBFs handle static and dynamic polygonal obstacles under partial observability and are integrated with inter-robot separation, elastic formation constraints, and goal CLFs in a unified local QP, extending CBF–QP methods to cluttered, dynamic environments with uncertain obstacles.

Furthermore, while MPC–CBF schemes (e.g., the dual MPC approach in [18]) offer strong predictive capabilities, their complexity scales with horizon length and team size, which can hinder fully decentralized real-time deployment, whereas our CLF–CBF–QP formulation uses lightweight per-agent QPs without horizon-based planning. Finally, hybrid and resilience-focused methods such as Saulnier et al. [19] and Cavorsi et al. [20] switch between a few modes or dynamically soften CBF constraints but do not structure multiple objectives (safety, connectivity, formation, goal reaching) into a unified hierarchy; our BT instead organizes several TV–CBFs and a CLF into a four-level "hierarchy of needs," [17] providing a richer high-level switching scheme that jointly handles resilience, connectivity, formation deformation/recovery, and obstacle avoidance in a decentralized formation controller.

III. Methodology

A. Graph Theory and Notation

Let $\mathcal{G} = (\mathcal{V}, \mathcal{E})$ be an undirected communication graph with $\mathcal{V} = \{1, \ldots, N\}$ and $\mathcal{E} \subseteq \mathcal{V} \times \mathcal{V}$. An edge $(i, j) \in \mathcal{E}$ indicates that robots i and j can exchange information. The neighbor set of robot i is defined as $\mathcal{N}_i := \{j \in \mathcal{V} \mid (i, j) \in \mathcal{E}\}$, with cardinality $|\mathcal{N}_i|$. Vectors are denoted in bold lowercase (e.g., $\mathbf{p}_i$) and matrices in bold uppercase. The position of robot i is $\mathbf{p}_i \in \mathbb{R}^2$, and $\mathbf{p}_{ij} := \mathbf{p}_i - \mathbf{p}_j$ denotes the relative position between robots i and j. The desired relative offset for each formation edge (i, j) is $\mathbf{d}_{ij} \in \mathbb{R}^2$.

B. Problem Setting

We consider a team of N mobile ground robots navigating a 2D environment with static and dynamic polygonal obstacles. Robots must maintain a desired formation, avoid collisions with obstacles and teammates, and reach a common goal using only local sensing and neighbor-to-neighbor communication in a fully decentralized manner. Each robot $i \in \{1, \ldots, N\}$ has single-integrator dynamics

$$\dot{p}_i = u_i, \quad p_i \in \mathbb{R}^2, \ u_i \in \mathbb{R}^2, \tag{1}$$

where p_i and u_i denote its position and control input. The communication network is modeled by an undirected graph $\mathcal{G} = (\mathcal{V}, \mathcal{E})$, where edges represent bidirectional information exchange among neighbors. Onboard range sensors detect static polygons $\mathcal{P}_{\text{stat}} \subset \mathbb{R}^2$ and time-varying polygons $\mathcal{P}_{\text{dyn}}(t) \subset \mathbb{R}^2$ with (possibly estimated) velocities $v_{\text{obs}}(t) \in \mathbb{R}^2$. The team executes a shared mission subject to four prioritized objectives in the following order: (i) safety (collision avoidance), (ii) preservation of connectivity, (iii) maintenance of the desired formation with adaptive tolerances, and (iv) convergence to mission goals. Among these, safety is the highest-priority requirement and dictates mode selection whenever imminent hazards are detected.

C. Control Barrier Function Based Quadratic Program

Consider the control-affine nonlinear system

$$\dot{\mathbf{x}} = f(\mathbf{x}) + g(\mathbf{x})\mathbf{u}, \tag{2}$$

where $\mathbf{x} \in \mathbb{R}^n$, $\mathbf{u} \in \mathbb{R}^m$, and f, g are locally Lipschitz. A continuously differentiable function $h : \mathbb{R}^n \to \mathbb{R}$ defines the safe set

$$\mathcal{C} := \{\mathbf{x} \mid h(\mathbf{x}) \geq 0\}. \tag{3}$$

The function h is a CBF if there exists an extended class-$\mathcal{K}$ function α such that

$$\sup_{\mathbf{u}} \left[L_f h(\mathbf{x}) + L_g h(\mathbf{x})\mathbf{u}\right] + \alpha(h(\mathbf{x})) \geq 0, \tag{4}$$

for all $\mathbf{x} \in \mathcal{C}$. In multi-robot systems, pairwise CBFs are often defined between agents i and j.

Lemma 1 [21, Thm. 4.1]: Let $h(\mathbf{x}_i, \mathbf{x}_j) = h(\mathbf{x}_j, \mathbf{x}_i)$ be a CBF with $\frac{\partial h}{\partial \mathbf{x}_i} g(\mathbf{x}_i) \neq 0$. Any Lipschitz controllers satisfying

$$\frac{\partial h}{\partial \mathbf{x}_i}\left(f(\mathbf{x}_i) + g(\mathbf{x}_i)\mathbf{u}_i\right) \geq -\alpha(h(\mathbf{x}_i, \mathbf{x}_j)) \tag{5}$$

render $\{h(\mathbf{x}_i, \mathbf{x}_j) \geq 0\}$ forward invariant.

Given a nominal input $\mathbf{u}_{\text{nom}}$, a minimally modified safe control is obtained from

$$\begin{aligned} \mathbf{u}^* = \arg\min_{\mathbf{u}} \quad & \|\mathbf{u} - \mathbf{u}_{\text{nom}}\|^2 \\ \text{s.t.} \quad & L_f h(\mathbf{x}) + L_g h(\mathbf{x})\mathbf{u} \geq -\alpha(h(\mathbf{x})). \end{aligned} \tag{6}$$

When multiple CBFs are active simultaneously, they are incorporated into a single QP, with slack variables added if necessary to ensure feasibility. Weights on these slack variables encode implicit task prioritization.

IV. Safety Guaranteed Distributed Formation Control Approach

A. Control Architecture

The control architecture, illustrated in Fig. 1, is organized into three modules. The **perception module** processes range measurements to estimate signed distances from its current position to each polygonal boundary and computes nearest-point gradients, and, when possible, obstacle motion. The **composed-constraint module** represents safety, formation, communication, and goal objectives as smooth, time-varying constraints with associated penalties. The **decision-making module**, implemented as a behavior tree (BT) [7], determines which constraints are active and how they are prioritized [17]. The BT evaluates predicates derived from local perception and neighbor-state information (e.g., *obstacle-too-close*, *link-loss-predicted*, *formation-slack-exceeded*) and selects operational modes such as nominal, recovery, or slack. This mapping enables conditional adjustment of non-safety objectives while always enforcing safety-first behavior.

At each control step, the BT specifies the active set of composed constraints, and a real-time optimizer running onboard computes the control input. Safety-related constraints are enforced as hard requirements or assigned the highest penalties, while communication and formation constraints are conditionally tightened or relaxed according to BT decisions. Goal tracking acts as the nominal objective, yet its influence is reduced whenever safety, communication, or formation constraints take precedence. All computations are fully decentralized and rely solely on local sensing and information exchanged with immediate neighbors, ensuring smooth transitions between nominal operation and recovery behaviors in dynamic, partially known environments.

Each robot independently computes its control input u_i by solving a local QP that enforces CBF constraints for safety and CLF constraints for convergence, using only information from local sensing and neighbor communication. The proposed method explicitly addresses three key aspects: collision avoidance, formation maintenance, and goal convergence.

B. Collision Avoidance

Collision avoidance is enforced both with respect to obstacles in the environment and with respect to other robots in the formation. Each robot $i \in \mathcal{V}$ uses its onboard range sensors to detect static and dynamic polygonal obstacles in its vicinity. For a static obstacle represented as a fixed polygon $\mathcal{P}_{\text{stat}} \subset \mathbb{R}^2$, we define a CBF

$$h_i^{\text{stat}}(p_i) = \text{dist}(p_i, \mathcal{P}_{\text{stat}}) - d_{\text{safe}}, \tag{7}$$

where $d_{\text{safe}} > 0$ is a pre-specified safety margin.

The forward invariance of the set $\{p_i \mid h_i^{\text{stat}} \geq 0\}$ is enforced through the CBF constraint

$$\nabla h_i^{\text{stat}}(p_i)^\top u_i \geq -\gamma_{\text{stat}} h_i^{\text{stat}}(p_i), \tag{8}$$

where $\gamma_{\text{stat}} > 0$ is a design parameter. For a dynamic obstacle modeled as a time-varying polygon $\mathcal{P}_{\text{dyn}}(t)$ with estimated boundary velocity $v_{\text{obs}}(t) \in \mathbb{R}^2$, the below signed distance function is used.

$$h_i^{\text{dyn}}(p_i, t) = \text{dist}(p_i, \mathcal{P}_{\text{dyn}}(t)) - d_{\text{safe}}, \tag{9}$$

and its time derivative accounts for obstacle motion as

$$\dot{h}_i^{\text{dyn}} = \nabla h_i(p_i)^\top (u_i - v_{\text{obs}}(t)). \tag{10}$$

The corresponding CBF constraint is

$$\nabla h_i(p_i)^\top u_i \geq \nabla h_i(p_i)^\top v_{\text{obs}}(t) - \gamma_{\text{dyn}} h_i^{\text{dyn}}(p_i, t), \tag{11}$$

where $\gamma_{\text{dyn}} > 0$ is the design parameter. Inter-robot collision avoidance is handled via pairwise CBFs. For each neighbor $j \in \mathcal{N}_i$, we define

$$h_{ij}(p_i, p_j) = \|p_i - p_j\|^2 - d_{\min}^2, \tag{12}$$

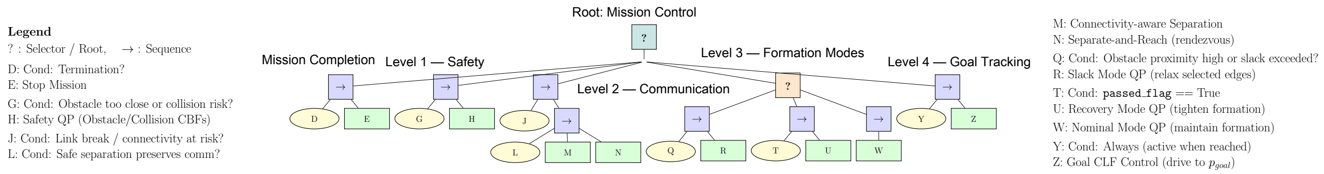

Fig. 2: Proposed behavior-tree–driven control framework for multi-robot formation. The decision logic is implemented via behavior trees to activate and prioritize constraints.

where $d_{\min} > 0$ is the minimum allowable separation. The safety constraint becomes

$$2(p_i - p_j)^\top u_i \geq -\gamma_{\rm col} h_{ij}(p_i, p_j), \tag{13}$$

where $\gamma_{\rm col} > 0$. The combination of (8), (11), and (13) guarantees that robot i maintains a safe distance from both obstacles and teammates at all times.

Remark 1: The CBF gain $\gamma > 0$ regulates how aggressively the controller pushes the state back toward the interior of the safe set: larger γ yields faster, more conservative avoidance (but can increase control effort and formation distortion), whereas smaller γ produces smoother motion at the cost of slower reactions near the boundary. The slack variables δ are introduced only for non-safety constraints (e.g., connectivity, formation) and are heavily penalized in the QP cost, so that they are used only when necessary to maintain feasibility in tight environments. Obstacle-avoidance CBFs are treated as hard constraints (no slack) in our implementation.

Remark 2: In this work, uncertainty is handled at the geometric level by using conservative time-varying CBFs built from estimated polygonal obstacle boundaries and bounded velocity estimates, rather than an explicit probabilistic or sensor-noise model. Extending the framework to chance-constrained or stochastic CBF formulations that directly account for perception uncertainty is an interesting avenue for future work.

C. Formation Maintenance

Formation maintenance is modeled via the communication graph $\mathcal{G}$. For each edge, the desired inter-robot distance is d_{ij}, but the actual distance may deviate within a time-varying tolerance $\epsilon_{ij}(t)$ to allow flexibility in navigating cluttered environments. The formation constraint is expressed as

$$(d_{ij} - \epsilon_{ij}(t))^2 \leq \|p_i - p_j\|^2 \leq (d_{ij} + \epsilon_{ij}(t))^2. \tag{14}$$

We define two CBFs to enforce the upper and lower bounds:

$$h_{ij}^{\rm up}(p_i, p_j) = (d_{ij} + \epsilon_{ij}(t))^2 - \|p_i - p_j\|^2, \tag{15}$$

$$h_{ij}^{\rm low}(p_i, p_j) = \|p_i - p_j\|^2 - (d_{ij} - \epsilon_{ij}(t))^2. \tag{16}$$

The upper bound prevents excessive stretching of the formation, while the lower bound constraint prevents the robots from collapsing into each other:

$$-2(p_i - p_j)^\top u_i \geq -\gamma_{\rm up} h_{ij}^{\rm up}(p_i, p_j), \tag{17}$$

$$2(p_i - p_j)^\top u_i \geq -\gamma_{\rm low} h_{ij}^{\rm low}(p_i, p_j). \tag{18}$$

Here $\gamma_{\rm up}, \gamma_{\rm low} > 0$ are design parameters. The tolerances $\epsilon_{ij}(t)$ can be adaptively increased in the vicinity of obstacles, allowing the formation to deform temporarily and then return to nominal spacing after obstacle clearance.

Algorithm 1 Composed-CBF–CLF–QP Control Algorithm

Input: x_i, neighbor states $\{x_j\}_{j\in\mathcal{N}_i}$, obstacle set $\mathcal{O}_i$, graph $\mathcal{G}$
Params: primitive CBFs $h_i^{\rm obs}$, $h_i^{\rm col}$, $h_{ij}^{\rm conn}$, $h_{ij}^{\rm form}$, CLF V_i, thresholds
while task not completed **do**
  Acquire / update x_i, $\{x_j\}_{j\in\mathcal{N}_i}$, $\mathcal{O}_i$
  Compute primitive CBF/CLF values and Lie derivatives
  Build level-wise composed TV-CBFs H_1 (safety), H_2 (connectivity), H_3 (formation)
  Initialize active constraint set $\mathcal{C} \leftarrow \emptyset$
  ▷ BT traversal (hierarchy of needs)
  if ObstacleTooClose($\mathcal{O}_i$) **then**
    $\mathcal{C} \leftarrow \{H_1\}$ ▷ Safety mode
  else if ConnectivityAtRisk($\mathcal{G}$) **then**
    $\mathcal{C} \leftarrow \{H_1, H_2\}$ ▷ Comm handler
  else if InNarrowPassage($\mathcal{O}_i$) **then**
    Activate SlackMode: relax $h_{ij}^{\rm form}$ (increase ε_{ij})
    $\mathcal{C} \leftarrow \{H_1, H_2\}$
  else if PassedCorridor() **then**
    Activate RecoveryMode: tighten $h_{ij}^{\rm form}$ (decrease ε_{ij})
    $\mathcal{C} \leftarrow \{H_1, H_2, H_3\}$
  else
    $\mathcal{C} \leftarrow \{H_1, H_2, H_3\}$ ▷ Nominal formation mode
  end if
  Add CLF V_i to objective (goal tracking)
  objective: minimize $\|u_i\|^2 + \sum_\ell \alpha_\ell \delta_\ell^2$
  subject to: $\dot{\tilde{H}}_i^\ell(u_i) + \kappa_\ell \tilde{H}_i^\ell \geq -\delta_\ell$, $-\dot{V}_i(u_i) \geq \gamma V_i - \delta_V$
  Solve QP $\Rightarrow u_i^\star$; apply $u_i \leftarrow u_i^\star$
end while

Remark 3: When a robot approaches an obstacle, the BT activates *SlackMode* and increases $\epsilon_{ij}(t)$ toward a prescribed upper bound $\epsilon_{ij}^{\max}$, allowing temporary formation deformation. After clearing the obstacle, the controller switches to *RecoveryMode* and smoothly decreases $\epsilon_{ij}(t)$ back to its nominal value $\epsilon_{ij}^{\rm nom}$, thereby restoring the desired formation.

D. Goal Convergence

The goal convergence task is handled via a CLF for each robot. Let $p_{\rm goal} \in \mathbb{R}^2$ denote the common goal location. The CLF and its constraints for robot i are expressed as

$$V_i(p_i) = \|p_i - p_{\rm goal}\|^2, \tag{19}$$

$$2(p_i - p_{\rm goal})^\top u_i \leq -\alpha V_i(p_i) + \delta_i^{\rm clf}, \tag{20}$$

where $\alpha > 0$ determines the rate of convergence and $\delta_i^{\rm clf} \geq 0$ is a slack variable to ensure feasibility when safety constraints are active.

E. Distributed Quadratic Program with Hierarchical Needs

We integrate the BT shown in Fig. 2 into a distributed control synthesis framework, inspired by the "hierarchy of needs" paradigm [6], [17]. Each level of the BT is modeled by a time-varying control barrier function (TV-CBF), which encodes a specific operational objective. The hierarchy is organized from the most fundamental to the most aspirational requirements: (1) safety through obstacle and collision avoidance, (2) communication preservation, (3) formation maintenance, and (4) goal convergence. This ordering ensures that higher-level objectives are pursued only when all lower-level constraints are satisfied. Let $H_\ell(p_i, t)$ denote the TV-CBF encoding the ℓ-th level needed for robot i at time t, constructed via smooth Boolean compositions of primitive CBFs for sub-tasks within that level, as in (8)–(19). Each H_ℓ is scaled, if necessary, using the sigmoid mapping [6]

$$\tilde{H}_\ell(p_i, t) = \frac{2}{1 + e^{-wH_\ell(p_i,t)}} - 1, \tag{21}$$

which preserves its 0-superlevel set while improving numerical conditioning. We define an indicator function $\Phi(\tilde{H}_\ell)$ that quantifies the degree to which lower-level needs are satisfied:

$$\Phi(\tilde{H}_\ell) = \begin{cases} 1, & \tilde{H}_\ell > b_\phi, \\ 3\left(\frac{\tilde{H}_\ell - a_\phi}{b_\phi - a_\phi}\right)^2 - 2\left(\frac{\tilde{H}_\ell - a_\phi}{b_\phi - a_\phi}\right)^3, & a_\phi \le \tilde{H}_\ell \le b_\phi, \\ 0, & \tilde{H}_\ell < a_\phi, \end{cases}$$

where $a_\phi < 0 < b_\phi$ are small margins to avoid chattering when approaching constraint boundaries. At each control step, robot i solves the hierarchical QP:

$$\begin{aligned} \min_{u_i,\, \delta_\ell} \quad & \|u_i - u_i^{\mathrm{nom}}\|^2 + \sum_{\ell=1}^{L-1} \kappa_{\ell+1}\delta_{\ell+1}^2 \qquad (22) \\ \text{s.t.} \quad & C(p_i, u_i, t; \tilde{H}_1) \ge 0, \\ & \left[\prod_{l=1}^{\ell} \Phi(\tilde{H}_l)\right] C(p_i, u_i, t; \tilde{H}_{\ell+1}) \ge -\delta_{\ell+1}, \\ & \delta_{\ell+1} \ge 0, \quad \forall \ell \in \{1, \ldots, L-1\}, \end{aligned}$$

where $C(\cdot)$ denotes the TV-CBF constraint as in (8)–(19) generalized to time-varying sets, u_i^{nom} is the nominal goal-seeking velocity, and $\kappa_{\ell+1} > 0$ penalizes relaxation of higher-level needs. The multiplicative term $\prod_{l=1}^{\ell} \Phi(\tilde{H}_l)$ ensures that the $(\ell+1)$-th level objective is enforced only when all lower-level needs are sufficiently satisfied.

F. Distributed QP-CBF Based Formation Control

Theorem 1: Consider N robots with single-integrator dynamics (1) in an environment with static and dynamic polygonal obstacles as in Section III. For each robot $i \in \mathcal{V}$, let $\{H_\ell^i(p_i, t)\}_{\ell=1}^L$ be the time-varying CBFs (TV–CBFs) obtained by smooth composition of the primitive CBFs for obstacle/collision avoidance, connectivity, and formation (cf. (7)–(18)), and let the hierarchical QP (21) use the indicators $\Phi(\tilde{H}_\ell^i)$ and a CLF $V_i(p_i)$. Assume: (A1) $p_i(0)$ lies in the interior of all safety and formation sets, i.e., $H_\ell^i(p_i(0), 0) > 0$ for $\ell = 1, 2, 3$. (A2) Each $H_\ell^i(\cdot, t)$ is C^1 in p_i and piecewise C^1 in t; polygonal obstacle boundary velocities are locally bounded. (A3) u_i^{nom} is locally Lipschitz and V_i is positive definite and radially unbounded. Then there exist design parameters $\gamma, \alpha > 0$ and penalty weights $\kappa_2, \ldots, \kappa_L \gg 1$ such that the QP solution $u_i^\star$ satisfies, for all $t \ge 0$:

1) (*Hierarchical safety*) The lowest-level TV–CBF set $\mathcal{C}_1^i(t) := \{p_i : H_1^i(p_i, t) \ge 0\}$ is forward invariant. Moreover, for any $k \in \{2, \ldots, L\}$, whenever there exists an input satisfying $C(p_i, u_i, t; H_\ell^i) \ge 0$ for $\ell = 1, \ldots, k$, the intersection $\bigcap_{\ell=1}^k \mathcal{C}_\ell^i(t)$ is also forward invariant under $u_i^\star$.

2) (*Elastic formation*) With BT-driven elastic bounds $\epsilon_{ij}(t)$ satisfying $0 < \epsilon_{ij}^{\min} \le \epsilon_{ij}(t) \le \epsilon_{ij}^{\max}$, all inter-robot distances remain within the time-varying tube $[d_{ij} - \epsilon_{ij}(t),\, d_{ij} + \epsilon_{ij}(t)]$, and converge back to the nominal tube corresponding to $\epsilon_{ij}^{\mathrm{nom}}$ once SlackMode is inactive.

3) (*Goal convergence*) If from some t_0 onward all safety and formation TV–CBF constraints are strictly satisfied (no safety-related slacks active), then the goal set $\{p_i : V_i(p_i) = 0\}$ is globally asymptotically stable for the closed-loop system under $u_i^\star$.

In particular, the closed-loop vector field $u^\star(p, t)$ is locally Lipschitz almost everywhere, so trajectories are well-defined and unique for all $t \ge 0$.

Proof: The closed-loop dynamics of robots are

$$\dot{p}_i = u_i^\star(p, t), \tag{23}$$

where $u_i^\star$ is the unique optimizer of the strictly convex QP (21). By (A2)–(A3), the QP data are locally Lipschitz in (p, t), so $u_i^\star$ is locally Lipschitz a.e., and standard ODE theory yields existence and uniqueness of trajectories. The TV–CBF constraints are

$$\dot{H}_\ell^i \ge -\gamma H_\ell^i - \delta_\ell. \tag{24}$$

Whenever $\delta_\ell = 0$, the time-varying Nagumo theorem gives forward invariance of $\mathcal{C}_\ell^i(t) := \{p_i : H_\ell^i \ge 0\}$. The hierarchical activation and the cost

$$J_i = \|u_i - u_i^{\mathrm{nom}}\|^2 + \sum_{\ell=1}^{L} \kappa_\ell \|\delta_\ell\|^2, \qquad 0 < \kappa_1 \ll \cdots \ll \kappa_L, \tag{25}$$

imply $\delta_\ell^\star = 0$ for all active levels whenever feasible, hence $\bigcap_\ell \mathcal{C}_\ell^i(t)$ is forward invariant. In particular, for each edge (i, j) the CBFs enforcing

$$d_{ij} - \epsilon_{ij}(t) \le \|p_i(t) - p_j(t)\| \le d_{ij} + \epsilon_{ij}(t) \tag{26}$$

render the elastic tube invariant; when SlackMode is inactive, $\epsilon_{ij}(t) \to \epsilon_{ij}^{\mathrm{nom}}$, so the formation converges to the nominal band. The CLF satisfies

$$\dot{V}_i \le -\alpha V_i + \delta_i^{\mathrm{clf}}. \tag{27}$$

Once safety and formation constraints are strictly satisfied, $\delta_i^{\mathrm{clf}} = 0$ is feasible and, for sufficiently large CLF weight, optimal, so $\dot{V}_i \le -\alpha V_i$ and

$$V_i(p_i(t)) \le V_i(p_i(t_0)) e^{-\alpha(t - t_0)}. \tag{28}$$

Thus $V_i \to 0$ and the goal set is globally asymptotically stable, which proves the theorem. ■

Remark 4: Theorem 1 shows that the proposed BT–coordinated hierarchical TV–CBF–CLF–QP framework enforces safety and connectivity as hard priorities, while allowing formation and goal objectives to be achieved whenever feasible. In particular, the result formalizes how the indicator-based hierarchy and penalty structure guarantee forward invariance of lower-level safety sets under dynamic polygonal obstacles, and enable adaptive relaxation and recovery of formation constraints without sacrificing stability.

V. EXPERIMENTS

We conducted experiments in the Robotarium simulation–hardware platform [22], which provides remote access to a multi-robot hardware testbed. A team of up to 4 robots was deployed in a 3m × 3m workspace, initially arranged in a square lattice configuration. All controllers were realized as per-robot convex QPs solved with OSQP and executed for $1{,}000$ time steps with $N = 4$ and $N = 8$ mobile robots. Robots are initialized in the left region of the testbed, making a square (or circular) formation, while the goal is set on the far right end $[1.5, 0]$ of the setup.

The proposed controller computes an analytic nominal velocity and projects it through a QP that enforces: (i) robust signed-distance obstacle CBFs for polygonal static obstacles and a limited set of linear moving obstacles, (ii) pairwise inter-robot CBFs with $d_{\text{safe}} = 0.1$, (iii) formation CBFs using offsets $\{[0.2, 0.2], [0.2, -0.2], [-0.2, -0.2], [-0.2, 0.2]\}$ with gains $\gamma_{\text{f\_rec}} = 100$ and $\gamma_{\text{f\_base}} = 30$, and (iv) a CLF constraint for goal tracking with slack $\epsilon_{\text{clf}} = 15$. Input bounds ($v_{\max} = 2.0$) and onboard mode logic (`recovery_mode`, `slack_mode`, `passed_flag`) switch between nominal and recovery behaviors in the BT when constraints activate.

To assess the effectiveness of the proposed decentralized Composed-CBF-CLF-QP framework, we benchmark it against three distributed CBF-based baselines: (i) an *Rigid/Elastic CBF-QP* [4], and (ii) a *Distributed CBF Controller* [8], (iii) a Distributed MPC controller inspired by dual-MPC schemes for multi-robot formation [18]. Comparisons are performed in identical Robotarium and simulation settings (same sensing, communication, per-robot QP solver, and initial conditions) and evaluated using: formation error (pairwise-distance), minimum robot–obstacle and inter-robot distances, and goal convergence time.

Fig. 3 summarizes a representative “narrow–passage” experiment in which a cluster of polygonal obstacles lies to the left of the workspace and two moving rectangular obstacles form a constrained corridor on the right. A team of $N = 4$ robots, initially in a square formation, must traverse this corridor to reach a common goal on the far right using only local sensing and neighbor-to-neighbor communication. In this setting we compare four controllers: (i) the proposed Composed–CBF–QP, (ii) the rigid/elastic CBF–QP baseline [4], (iii) the distributed CBF controller of [8], and (iv) the Distributed MPC controller [18].

For all methods, Fig. 4(a) reports, for each robot, the minimum measured distance to the nearest static or dynamic obstacle over time, while Fig. 4(b) shows the evolution of inter-robot distances, and Fig. 4(c) depicts the target-tracking and formation-error trajectories, respectively. The proposed Composed–CBF–QP maintains robot–obstacle distances strictly above the safety buffer ($d_{\text{obs,safe}} = 0.08\,\text{m}$) for both polygonal and moving rectangular obstacles, without the excessively conservative clearances exhibited by the distributed-CBF baseline. This indicates that the signed-distance CBFs built directly from polygonal geometry are effective at enforcing safety in cluttered, dynamic environments. At the same time, the proposed controller preserves inter-agent distances close to their nominal values, with smaller transients and faster post-avoidance recovery than both CBF-based baselines; this is reflected in the lower steady-state formation error and quicker return to the desired formation tube after the corridor is cleared.

TABLE I: Performance comparison for different numbers of dynamic obstacles and robots. NR: goal not reached within horizon. Fail: deadlock occurred. Negative minimum distance indicates a collision. O/N=Number of Obstacles/Robots.

Scenario	Controller	Time-to-goal (s)	Final form. error (m)	Avg form. error (m)	Min d_{ro} (m)	Min d_{rr} (m)	Avg solve time (ms)	Max solve time (ms)
O=2, N=4	Dist. MPC [18]	62.2	0	0.269	0	0.036	440.6	772.7
	Dist. CBF [8]	62.0	0.004	0.191	-0.116	0.118	35.0	73.8
	CBF-CLF-QP [ours]	57.0	0.153	0.464	0	0.076	51.5	181.5
	Rigid/Elastic CBF-QP [4]	45.1	0.006	0.491	-0.173	0.152	57.0	103.7
O=4, N=4	Dist. MPC [18]	56.5	0	0.227	0	0.009	480.4	1094.7
	Dist. CBF [8]	NR	0.971	0.506	-0.116	0.094	35.8	69.9
	CBF-CLF-QP [ours]	75.0	0.150	1.226	0	0.008	56.0	162.0
	Rigid/Elastic CBF-QP [4]	87.6	0.061	0.505	-0.194	0.200	60.4	97.9
O=6, N=4	Dist. MPC [18]	54.4	0.001	0.220	0	0.036	562.4	1109.9
	Dist. CBF [8]	NR	2.766	1.753	-0.182	0.100	41.0	75.8
	CBF-CLF-QP [ours]	71.3	0.149	0.476	0	0.179	59.2	193.8
	Rigid/Elastic CBF-QP [4]	Fail	–	–	–	–	–	–
O=2, N=8	Dist. MPC [18]	82.5	0	0.252	0	0.004	1581.3	277810.0
	Dist. CBF [8]	NR	3.910	1.815	-0.256	0.031	87.7	139.6
	CBF-CLF-QP [ours]	94.6	0.191	0.862	0.011	0.010	119.7	301.1
	Rigid/Elastic CBF-QP [4]	Fail	–	–	–	–	–	–
O=2, N=20	Dist. MPC [18]	79.6	0	0.399	0	0.001	7411.5	9569.7
	Dist. CBF [8]	NR	5.120	2.231	-0.277	0.002	346.7	518.4
	CBF-CLF-QP [ours]	98.0	1.721	1.941	0	0	538.7	770.2
	Rigid/Elastic CBF-QP [4]	Fail	–	–	–	–	–	–

In the corridor scenario, Distributed MPC often achieves a time-to-goal comparable to, or slightly faster than, the CBF-based controllers (cf. Table I), since the predictive planner can exploit look-ahead to commit to aggressive maneuvers once a feasible open-loop path is found. However, this performance comes at a substantial computational cost: Fig. 4(c) shows that the per-step solve time for the Distributed MPC controller is on the order of 0.4–$0.8\,\text{s}$, with occasional spikes exceeding $1\,\text{s}$, whereas the proposed Composed–CBF–QP and the two CBF-based baselines remain in the tens-of-milliseconds range (average ≈ 50–$60\,\text{ms}$ per step for Composed–CBF–QP, and even lower for the purely distributed CBF controller). As summarized in Table I, this corresponds to roughly an order-of-magnitude gap in computational burden, which can be prohibitive for real-time, on-board deployment on resource-limited platforms.

Qualitatively, the differences between the methods can be interpreted as follows. The rigid/elastic CBF–QP preserves formation more tightly than the distributed-CBF controller but tends to exhibit oscillations and chattering near the corridor entrance, occasionally stretching or compressing specific edges as it negotiates the tight passage. The distributed-CBF baseline, which does not include an explicit formation-restoration mechanism, often either takes overly conservative detours or fails to recover the nominal formation once obstacles are cleared. By contrast, the proposed Composed–CBF–QP embeds a distributed Slack/Recovery mech-

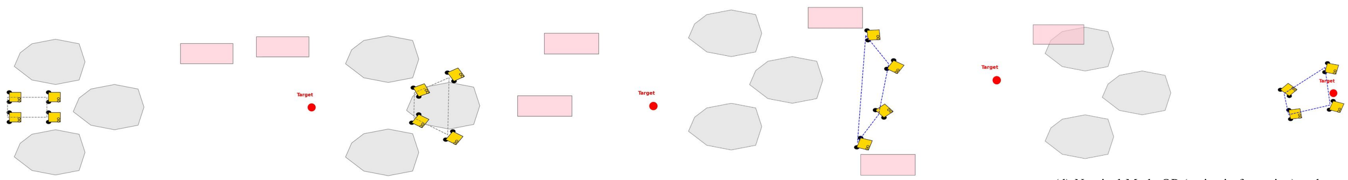

(a) Initial Formation (b) Slack Mode QP (relax selected edges) (c) Recovery Mode QP (tighten formation) (d) Nominal Mode QP (maintain formation) and target-reaching

Fig. 3: Illustration of experiments in the Robotarium, showing the evolution of the robot trajectories in the presence of both static and dynamic obstacles.

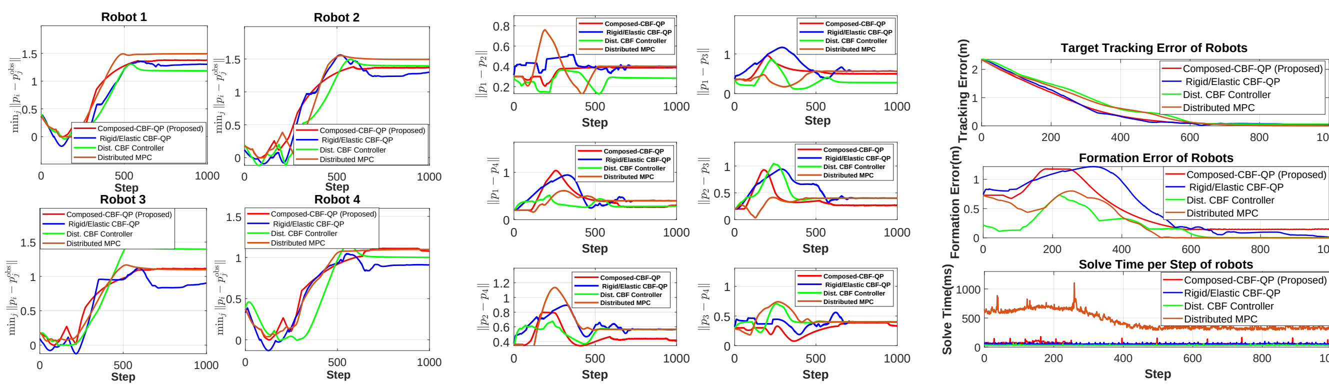

(a) Obstacle avoidance performance (b) Avoiding inter-robot collisions (c) Task-related errors: Formation keeping and target tracking

Fig. 4: Performance results illustrating (a) minimum robot–obstacle distances, (b) inter-robot distances, and (c) target tracking, formation error, and computation time in the presence of both static and dynamic obstacles in unknown environments.

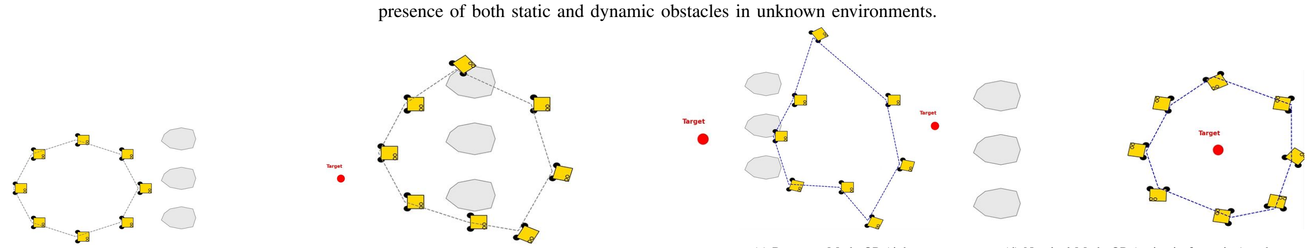

(a) Initial Formation (b) Slack Mode QP (relax selected edges) (c) Recovery Mode QP (tighten formation) (d) Nominal Mode QP (maintain formation) and target-reaching

Fig. 5: Illustration of experiments in the Robotarium, showing the evolution of the $N = 8$ robot trajectories in the presence of static obstacles with unknown geometry.

anism driven by the BT hierarchy: selected formation edges are temporarily relaxed in *Slack Mode* to allow the robots to squeeze through the narrow corridor, and are then tightened in *Recovery Mode* once the *passed* condition is satisfied. This coordinated deformation and restoration of the formation yields the smallest post-avoidance formation error among the CBF-based controllers, while achieving goal-convergence times comparable to Distributed MPC but with significantly lower computation time. Overall, the results highlight that the proposed BT–coordinated Composed–CBF–QP offers a favorable trade-off between safety, formation integrity, and computational efficiency in environments with static and dynamic obstacles of unknown geometry.

Figs. 5 and 6 demonstrate the scalability of the proposed Composed-CBF-CLF-QP framework with $N = 8$ robots in a circular formation navigating toward a common goal in a cluttered environment. As shown in Fig. 6(a), inter-robot distances remain bounded and close to nominal values, with only brief transients near obstacles. The minimum robot–obstacle distances in Fig. 6(b) stay above the safety threshold, confirming robust collision avoidance. Formation errors in Fig. 6(d) exhibit short deviations during obstacle encounters but quickly recover due to the Slack/Recovery mechanism, resulting in low steady-state error. Finally, Fig. 6(c) shows rapid convergence of the tracking error, indicating that performance is preserved as team size increases.

Table I highlights the scalability of the proposed CBF composition architecture as both obstacle density and team size increase. Across all scenarios, including the most demanding case with 2 obstacles and 20 robots, our method consistently reaches the goal without deadlock or "NR" cases, maintains safe robot–obstacle and inter–robot distances, and keeps the average solve time in the sub–100 ms range, which is compatible with real-time execution. In contrast, the rigid/elastic CBF–QP baseline fails or becomes unstable in cluttered environments (e.g., 6 obstacles and 4 robots), and the distributed CBF controller exhibits large formation errors and non-reachability for larger teams (8–20 robots). Distributed MPC often achieves favorable time-to-goal, but its average and worst-case solve times grow rapidly with the number of robots—reaching several seconds per step in the 20-robot case—making it significantly less scalable computationally than our approach. Overall, the table shows that Composed–CBF–QP offers a more favorable trade-off among safety, formation tracking, and computational cost as the number of robots and obstacles increases.

To validate the proposed decentralized Composed-CBF-

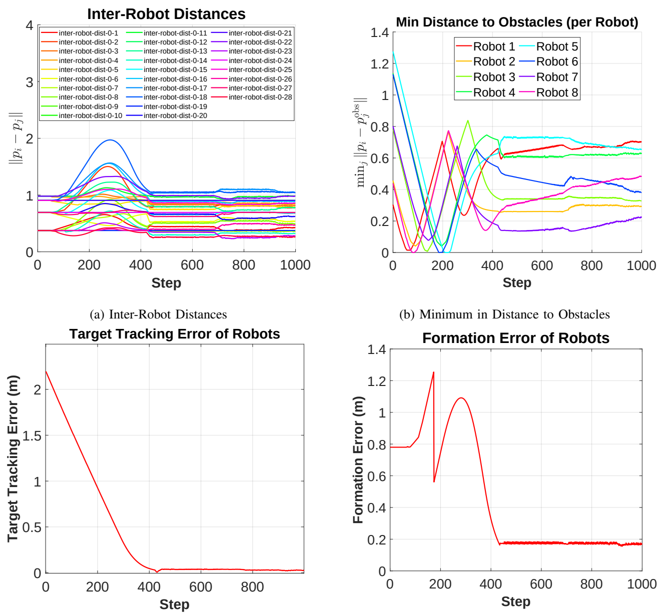

(a) Inter-Robot Distances

(b) Minimum in Distance to Obstacles

(c) Target Tracking Error of Robots

(d) Formation Error of Robots

Fig. 6: Scalability analysis of the proposed method with $n = 8$ in the presence of static obstacles with unknown geometry.

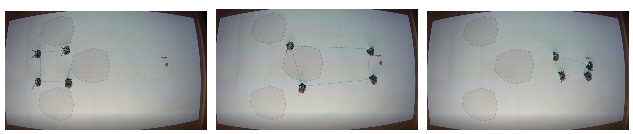

Fig. 7: Demonstration in Robotarium hardware platform, showing the evolution of the robot trajectories in the presence of static obstacles with unknown geometry.

CLF-QP framework, hardware experiments were conducted on the Robotarium platform. A team of robots maintained the desired formation while navigating environments with static obstacles of unknown geometry. Actuator limits were explicitly included in the controller to ensure feasibility on real hardware. As shown in Fig. 7, the robots adapted their trajectories in real time to avoid collisions, respect actuator constraints, and preserve formation, demonstrating the practicality and robustness of the approach.

VI. Conclusion

This paper presented a decentralized Composed-CBF-CLF-QP framework for safe and adaptive multi-robot formation control in uncertain and cluttered environments. By integrating multiple CBFs and a CLF within a BT-coordinated quadratic program, the approach ensures safety, connectivity, formation maintenance, and goal convergence under actuator constraints. Experiment results in static and dynamic scenarios showed tighter formations, faster recovery, and less conservative navigation compared to distributed CBF baselines. Scalability analysis confirmed the efficiency and robustness of the per-robot decentralized architecture, and hardware experiments on the Robotarium platform demonstrated its feasibility under real-world sensing, actuation, and communication limitations.

References

[1] A. R. Vetrella, G. Fasano, D. Accardo, and A. Moccia, "Differential gnss and vision-based tracking to improve navigation performance in cooperative multi-uav systems," *Sensors*, vol. 16, no. 12, p. 2164, 2016.

[2] M. Radmanesh and M. Kumar, "Flight formation of uavs in presence of moving obstacles using fast-dynamic mixed integer linear programming," *Aerospace Science and Technology*, vol. 50, pp. 149–160, 2016.

[3] J. Alonso-Mora, S. Baker, and D. Rus, "Multi-robot formation control and object transport in dynamic environments via constrained optimization," *The International Journal of Robotics Research*, vol. 36, no. 9, pp. 1000–1021, August 2017.

[4] H. Pham, N. Ranasinghe, D. Le, M. W. S. Atman, and A. Gusrialdi, "Safety-guaranteed distributed formation control of multi-robot systems over graphs with rigid and elastic edges," *IEEE Robot. Autom. Lett.*, vol. 9, no. 11, pp. 10 240–10 247, Nov. 2024.

[5] P. Ogren, M. Egerstedt, and X. Hu, "A control lyapunov function approach to multi-agent coordination," in *Proc. IEEE Conf. Decis. Control (CDC)*, vol. 2. IEEE, 2001, pp. 1150–1155.

[6] R. Lin and M. Egerstedt, ""hierarchy of needs" for robots: Control synthesis for compositions of hierarchical, complex objectives," in *2025 IEEE Int. Conf. Robot. Autom. (ICRA)*, 2025, pp. 7682–7688.

[7] P. Ögren and C. I. Sprague, "Behavior trees in robot control systems," *Annual Review of Control, Robotics, and Autonomous Systems*, vol. 5, no. 1, pp. 81–107, 2022.

[8] P. Mestres, C. Nieto-Granda, and J. Cortés, "Distributed safe navigation of multi-agent systems using control barrier function-based controllers," *IEEE Robot. Autom. Lett.*, vol. 9, no. 7, pp. 6760–6767, Jul. 2024.

[9] G. Notomista and M. Egerstedt, "Constraint-driven coordinated control of multi-robot systems," in *Proc. Amer. Control Conf. (ACC)*, Philadelphia, PA, USA, 2019, pp. 1990–1996.

[10] A. Pallar, G. Li, M. Sarvaiya, and G. Loianno, "Optimal trajectory planning for cooperative manipulation with multiple quadrotors using control barrier functions," *arXiv preprint arXiv:2503.01892*, March 2025. [Online]. Available: https://arxiv.org/abs/2503.01892

[11] S. Zhao, "Affine formation maneuver control of multiagent systems," *IEEE Trans. Autom. Control*, vol. 63, no. 12, pp. 4140–4155, 2018.

[12] X. Fang and L. Xie, "Distributed formation maneuver control using complex laplacian," *IEEE Trans. Autom. Control*, vol. 69, no. 3, pp. 1850–1857, Mar. 2024.

[13] H. G. de Marina, J. J. Castellanos, and W. Yao, "Leaderless collective motions in affine formation control," in *Proc. IEEE Conf. Decis. Control (CDC)*, Austin, TX, USA, 2021, pp. 6433–6438.

[14] P. Glotfelter, I. Buckley, and M. Egerstedt, "Hybrid nonsmooth barrier functions with applications to provably safe and composable collision avoidance for robotic systems," *IEEE Robot. Autom. Lett.*, vol. 4, no. 2, pp. 1303–1310, Apr. 2019.

[15] S. Keyumarsi, M. W. S. Atman, and A. Gusrialdi, "Lidar-based online control barrier function synthesis for safe navigation in unknown environments," *IEEE Robot. Autom. Lett.*, vol. 9, no. 2, pp. 1043–1050, Feb. 2024.

[16] A. D. Ames, X. Xu, J. W. Grizzle, and P. Tabuada, "Control barrier function based quadratic programs for safety-critical systems," *IEEE Trans. Autom. Control*, vol. 62, no. 8, pp. 3861–3876, 2017.

[17] Q. Yang and R. Parasuraman, "Hierarchical needs based self-adaptive framework for cooperative multi-robot system," in *Proc. IEEE Int. Conf. Syst., Man, Cybern. (SMC)*, 2020, pp. 2991–2998.

[18] S. Wang, Y. Wang, Z. Miao, X. Wang, and W. He, "Dual model predictive control of multiple quadrotors with formation maintenance and collision avoidance," *IEEE Trans. Ind. Electron.*, vol. 71, no. 12, pp. 16 037–16 046, Dec. 2024.

[19] K. Saulnier, D. Saldaña, A. Prorok, G. J. Pappas, and V. Kumar, "Resilient flocking for mobile robot teams," *IEEE Robot. Autom. Lett.*, vol. 2, no. 2, pp. 1039–1046, Apr. 2017.

[20] M. Cavorsi, L. Sabattini, and S. Gil, "Multirobot adversarial resilience using control barrier functions," *IEEE Trans. Robot.*, vol. 40, pp. 797–815, 2024.

[21] T. Ibuki, T. Hirano, R. Funada, and M. Sampei, "Optimization-based distributed safety control with applications to collision avoidance for mobile robotic networks," *Advanced Robotics*, vol. 37, pp. 87–98, Jan. 2023.

[22] S. Wilson, P. Glotfelter, L. Wang, S. Mayya, G. Notomista, M. Mote, and M. Egerstedt, "The robotarium: Globally impactful opportunities, challenges, and lessons learned in remote-access, distributed control of multirobot systems," *IEEE Control Syst. Mag.*, vol. 40, no. 1, pp. 26–44, 2020.